doi:10.1016/j.jmb.2006.07.007 J. Mol. Biol. (2006) 362, 430–440

JMB

Available online at www.sciencedirect.com

ScienceDirect

ELSEVIER

Structural and Functional Analysis of *Saccharomyces cerevisiae* Mob1

Serge Mrkobrada[1,2], Lorrie Boucher[1,2], Derek F. J. Ceccarelli[1] Mike Tyers[1,2]* and Frank Sicheri[1,2]*

[1]*Program in Molecular Biology and Cancer, Samuel Lunenfeld Research Institute, Mount Sinai Hospital, 600 University Avenue, Toronto, Ontario Canada M5G 1X5*

[2]*Department of Molecular and Medical Genetics, University of Toronto, Toronto, Ontario Canada M5S 1A8*

**Corresponding authors*

The Mob proteins function as activator subunits for the Dbf2/Dbf20 family of protein kinases. Human and *Xenopus* Mob1 protein structures corresponding to the most conserved C-terminal core, but lacking the variable N-terminal region, have been reported and provide a framework for understanding the mechanism of Dbf2/Dbf20 regulation. Here, we report the 2.0 Å X-ray crystal structure of *Saccharomyces cerevisiae* Mob1 containing both the conserved C-terminal core and the variable N-terminal region. Within the N-terminal region, three novel structural elements are observed; namely, an α-helix denoted H0, a strand-like element denoted S0 and a short β strand denoted S-1. Helix H0 associates in an intermolecular manner with a second Mob1 molecule to form a Mob1 homodimer. Strand S0 binds to the core domain in an intramolecular manner across a putative Dbf2 binding site mapped by Mob1 temperature-sensitive alleles and NMR binding experiments. *In vivo* functional analysis demonstrates that Mob1 mutants that target helix H0 or its reciprocal binding site are biologically compromised. The N-terminal region of Mob1 thus contains structural elements that are functionally important.

Keywords: mitotic exit network; Mob1; X-ray crystallography; cell cycle; *Saccharomyces cerevisiae*

Introduction

The Mob proteins are a small family of highly conserved, non-catalytic proteins that are found in all eukaryotes.[1] In fungi, there are two Mob proteins, Mob1 and Mob2, while an expansion in metazoans gives rise to six in human (as per cDNAs), four in *Drosophila melanogaster*, and four in *Caenorhabditis elegans*. Mob proteins play critical roles in cell-cycle regulation and function chiefly by interacting with and activating the Dbf2-related protein kinases.[2–4] This subfamily of serine/threonine kinases includes Dbf2, Dbf20 and Cbk1 in *S. cerevisiae*, Ndr1, Ndr2, Lats1 and Lats2 in human, Warts (aka dLats) and Trk (aka dNdr) in *D. melanogaster* and Sax1 (aka ceNdr) and a hypothetical Lats homolog (accession number O45797) from *C. elegans*. Like their Mob protein partners, this subfamily of protein kinases regulate cell growth, cell division and cell morphology.[5–7] The functional co-dependence and cell-cycle regulation of the Mob and Dbf2-like proteins is reminiscent of how cyclins bind and regulate cyclin dependant kinases (CDK).[4,8,9]

In *S. cerevisiae*, exit from mitosis coincides with a transition from a state of high CDK activity to a state of low CDK activity.[10,11] Mob1 and the related kinases Dbf2 and Dbf20 are part of the regulatory signaling cascade that governs this transition, referred to as the mitotic exit network (MEN).[12] In late anaphase, the Mob1-bound form of Dbf2 is phosphorylated and activated by the upstream kinase Cdc15.[4] Activation of the MEN leads to the release of the dual specificity phosphatase Cdc14 from the nucleolus. Mob2, in contrast binds and regulates Cbk1, a component of the RAM signaling network that acts chiefly to localize and activate Ace2 in the daughter cell nucleus.[13,14] While Mob1 has been shown by two-hybrid analysis to bind Cbk1 kinase, the function of this interaction is not known.[15]

Mob1 function is less well understood in metazoans. In humans, two of the six Mob proteins, Mob1B and Mob2, have been shown to bind Ndr1 and Ndr2.[16] The binding of human Mob2 to Ndr1 and Ndr2 leads to kinase activation, while co-expression

Abbreviation used: CDK, cyclin dependant kinases.

E-mail addresses of the corresponding authors: tyers@mshri.on.ca; sicheri@mshri.on.ca

of Ndr1 or Ndr2 alters Mob2 localization from the nucleus dramatically.[16] However, Mob1b localization does not seem to be affected. *D. melanogaster* Mob1 (Mats) physically and/or functionally interacts with both Wts and Trc kinases and facilitates Wts activation.[17,18] Importantly, the loss of dMob1 function in *D. melanogaster* results in increased cell proliferation, a reduction of apoptosis, and induction of tissue overgrowth.[17] As Wts loss of function mutations display the same phenotypes, it is likely that dMob1 and Wts function in the same pathway. A role for the Mob/Dbf2 kinases in tumor suppression is suggested also by the finding that mice deficient in mLats1 develop soft-tissue sarcoma and ovarian tumors,[19] and that mLats2 mutant embryos display overgrowth in mesodermally derived tissues.[20] Furthermore, analysis of cDNA sequences from mouse and human tumor cell lines has revealed mutations in Mob1, consistent with a tumor suppressor function for Mob1.[17]

Mob proteins are approximately 210 to 240 amino acid residues in length, with the exception of *S. cereviae* Mob1, which has a further 78 residue N-terminal extension not conserved or even present in the closely related fungal proteins (Figure 1). The structure of a Dbf2-like family kinase either alone or in complex with a partner Mob protein has yet to be determined. However, structures of human and *Xenopus* Mob1 fragments corresponding to the most highly conserved C-terminal region have been determined.[21,22] Both structures correspond to protease-resistant cores (analogous to *S. cerevisae* Mob1$^{133\text{-}314}$) that possess an α-helical architecture common to all Mob proteins. We refer to this region as the core domain (Figure 1).

While less conserved than the core domain, the N-terminal region of Mob proteins is conserved within subgroups of Mob proteins (Figure 1, and discussed below). The N-terminal region appears to be functionally important, because ScMob1$^{79\text{-}314}$ is able to complement a *mob1* deletion, whereas the core domain, ScMob1,$^{145\text{-}314}$ is functionally compromised.[2] As structural information relating to the N-terminal region of Mob proteins is lacking, we have determined the X-ray crystal structure of *S. cerevisiae* Mob1.$^{79\text{-}314}$ Unlike previously determined Mob1 core structures, ScMob1$^{79\text{-}314}$ is a dimer in solution and in crystal form. Three portions of the conserved N-terminal region adopt structured conformations that contribute, in part, to Mob1 homodimerization *in vitro*. Thus, the conserved N-terminal region may help to differentiate specific functions of the Mob proteins.

Results

Mob protein subgroups

Alignment of the core domain of Mob proteins from yeast to human identifies three distinct groups defined, in part, by similarity between the conserved N-terminal region (Figure 1; Supplementary Data Figure 1). On the basis of the position of the archetypal members ScMob1 and Mob2 within the clustered groups, we refer to the groups loosely as Mob1-like, Mob2-like and Mob3-like. Within the Mob1-like group are two subgroups (A and B), with the Mob1A subgroup containing the clear-cut orthologues of ScMob1 in fungal species and a single Mob protein from *Homo sapiens* and *Drosophila melanogaster*. The Mob1B subgroup contains one or more Mob proteins from each metazoan species analyzed. Two distinct subgroups are apparent in the Mob2-like group, with one subgroup (Mob2B) consisting strictly of the fungal orthologues of ScMob2 and the second (Mob2A) containing metazoan orthologues. The Mob3-like group is the most divergent and consists of a single protein from each metazoan species analyzed. These groupings provide a framework for the discussion of the structure/function analysis detailed below.

Structure determination of ScMob1$^{79\text{-}314}$

ScMob1$^{79\text{-}314}$ contains the conserved Mob core and the N-terminal region not present in previous Mob protein structure analyses (residues 79–132), but not the extreme N terminus unique to *S. cerevisiae* (residues 1–78). ScMob1$^{79\text{-}314}$ was expressed in bacteria as a glutathione-*S*-transferase (GST) fusion and purified to homogeneity (see Materials and Methods). Protein crystals of the space group *C*2 were obtained in 0.1 M MES (pH6.0), 1.24 M ammonium sulfate. Representative crystals diffracted to 2.0 Å, which facilitated a structure determination by the SeMet multiple anomalous dispersion method (see Materials and Methods).

The ScMob1 core structure (residues 145–314) is very similar to the previously reported human and *Xenopus* Mob1 core structures (RMSD *versus* human Mob1 = 0.86 Å; RMSD *versus Xenopus* Mob1 = 1.46 Å) with small differences occurring in the loop regions (Figure 3(a)). Unlike previously reported Mob1 core structures, ScMob1$^{79\text{-}314}$ forms an interdigitated dimer within the crystal environment. Consistently, static light-scattering analysis indicated that the protein forms a dimer at the concentrations employed for crystallization trials at 25 mg/ml (Supplementary Data Figure 2). The protomer structure consists of a Mob1 core preceded by three structural elements not observed in previous structural analyses; namely, a short β strand region denoted S-1 (residues 81–85), an extended strand region denoted S0 (residues 98–112) and an α-helix denoted H0 (residues 126–139) (Figure 2). In the experimentally determined maps, the electron density for the novel N-terminal structural elements is well defined and of a quality similar to that observed for the Mob1 core (Supplementary Data, Figure 4). Accordingly, the average side-chain *B*-factors for strand S-1 (30 Å^2), strand S0 (21 Å^2), and helix H0 (31 Å^2) are similar to the average side-chain *B*-factors for the Mob1 core (24 Å^2). One notable difference in the ScMob1 core structure is the

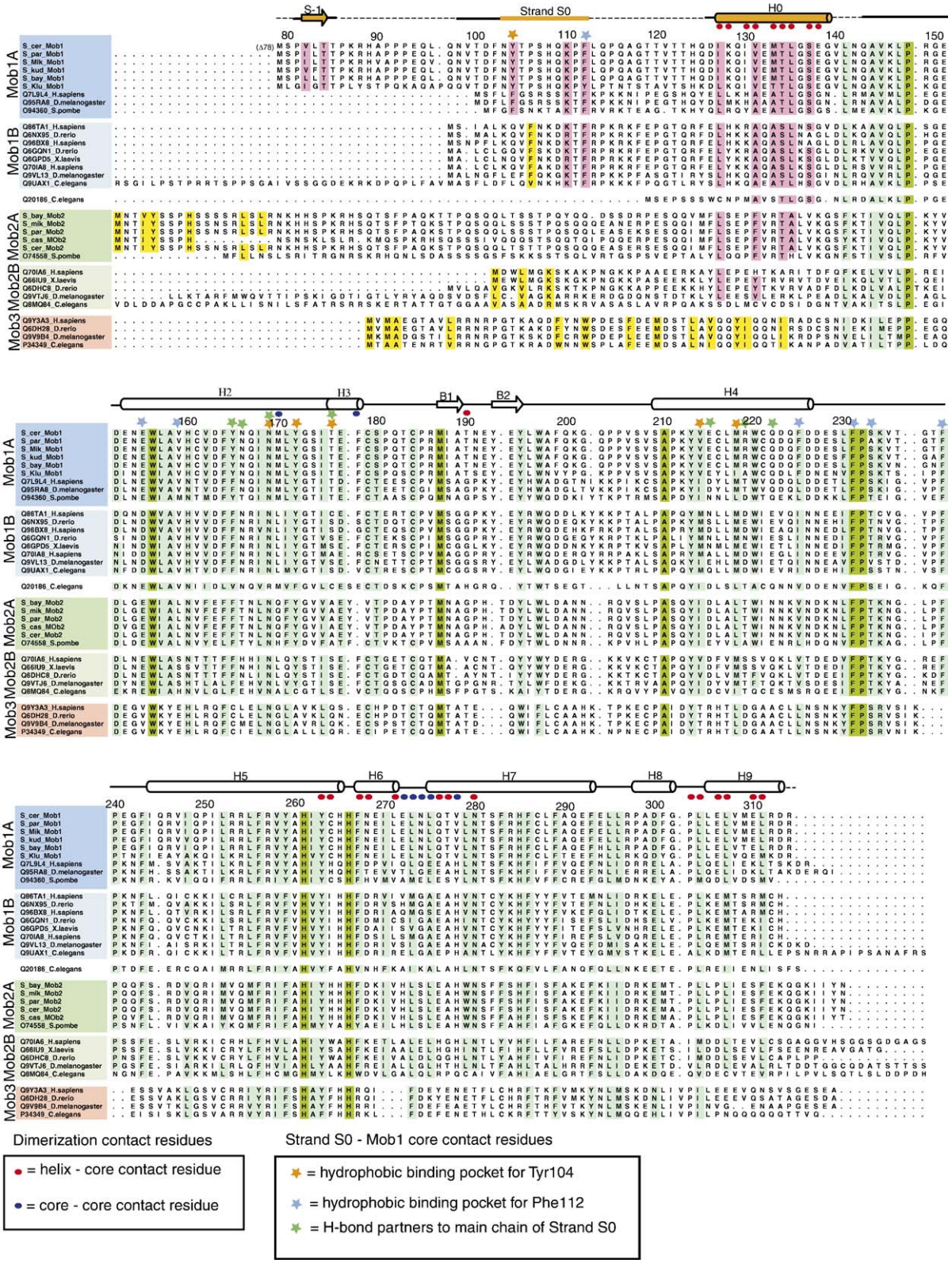

Figure 1. Structure-based sequence alignment of the Mob protein family consisting of fungal (*S. cerevisiae*, *S. paradoxus*, *S. mitakae*, *S. kluyveri*, *S. bayanus*, *S. paradoxus*, *S. castellii*, *S. pombe*) and metazoan (*H. sapiens*, *X. laevis*, *D. rerio*, *D. melanogaster*, *C. elegans*) Mob proteins, which are grouped and aligned on the basis of sequence similarities within the core region. Three main groups, Mob1, Mob2 and Mob3, are revealed. The Mob1 and Mob2 groups are further subdivided into the Mob1A, Mob1B, Mob2A and Mob2B subgroups. Invariant core residues are highlighted in dark green, and conserved Mob core residues are highlighted in light green. In the N-terminal region, highly conserved Mob1 residues in helix H0 and strand S0 are colored pink, and subgroup-specific conserved residues are colored yellow. The secondary structure of the *S. cerevisae* Mob1$_{79\text{-}314}$ is indicated above the alignment with the two novel structural elements (strand S0 and helix H0) highlighted in orange. Broken lines represent regions that could not be modeled due to lack of electron density.

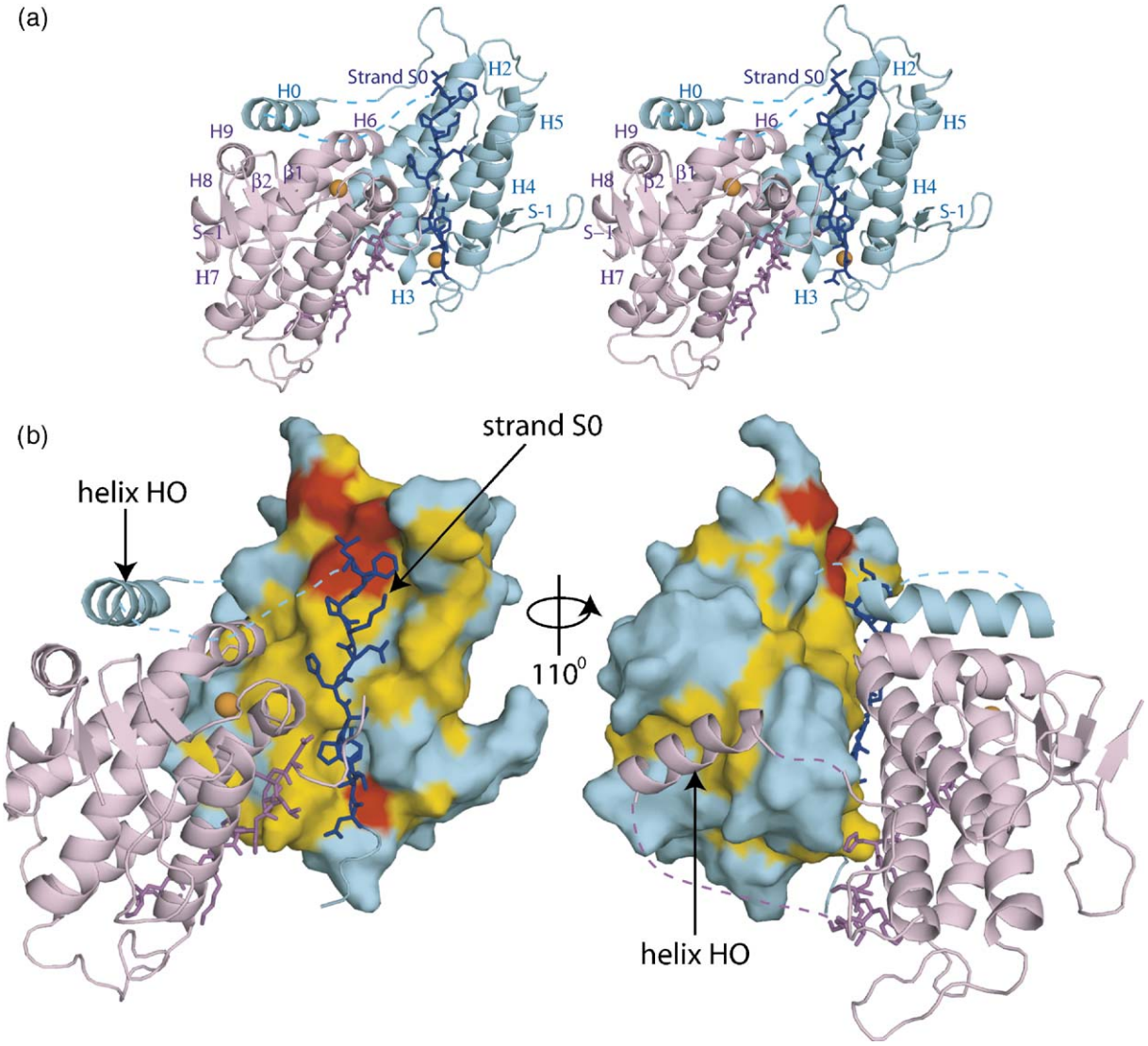

Figure 2. Structure of the *S. cerevisae* Mob1$^{79\text{-}314}$ homodimer. (a) Stereo representation of the ScMob1$^{79\text{-}314}$ homodimer. One molecule of the homodimer is shown in blue and the other is in pink. ScMob1$^{79\text{-}314}$ secondary structure elements are labeled. Regions that could not be modeled are represented as broken lines. The Mob1-bound Zn atom is represented as an orange sphere. (b) Surface representation of ScMob1$^{79\text{-}314}$. Invariant residues in eukaryotic and fungal Mob1A proteins are shown in yellow. Mob1 temperature-sensitive alleles are highlighted in red.[22] The figure on the left is shown in the same orientation as in (a), whereas the figure on the right represents a 110° counterclockwise rotation about the *y*-axis.

absence of a short 3_{10} helix H1, found at the N terminus of both human and *Xenopus* Mob1 structures (Figure 3(a)). In the ScMob1 structure, this region is largely disordered. In brief, the core domain consists of seven α helices, one 3_{10} helix, and one β hairpin. The four longest α-helices, H2, H4, H5 and H7, form a central helical bundle, which is capped on one end by two shorter α-helices, H3 and H6, and a β hairpin bound to a zinc ion. Helices H8 and H9 pack laterally against the side of the four helix bundle. The zinc ion is present also in hMob1 and XMob1 core structures. In the ScMob1 structure, the zinc-binding pocket is composed by Cys179, Cys184, His261 and His266 side-chains (Figure 3(b)). His261 and His266 reside within the helix H5-H6 linker and are invariant across all Mob groups. In contrast, Cys179 and Cys184, which reside within the helix H2-β1 linker, are absent from the Mob2A subgroup, suggesting that Mob2A members may not bind zinc or bind zinc through an alternative mechanism. The ScMob1 zinc-binding pocket is virtually identical with that of the human Mob1 protein (Figure 3(b)).

Of particular note, the N-terminal region strand S0 binds to the Mob1 core in an intramolecular manner across a conserved surface composed of helices H2, H3 and H4, as well as the H4-H5 linker. In contrast, the N-terminal region helix H0 binds in an intermolecular fashion to the conserved surface of an opposing Mob1 core composed of helices H5, H6, H7, H9 as well as the H8-H9 linker. The linker between the Mob1 core and helix H0 (residues 140–142), and the linker between helix H0 and strand S0 (residues 113–125) are disordered and hence could not be modeled in the crystal structure. Importantly, the linker between helix H0 and the Mob1 core is not

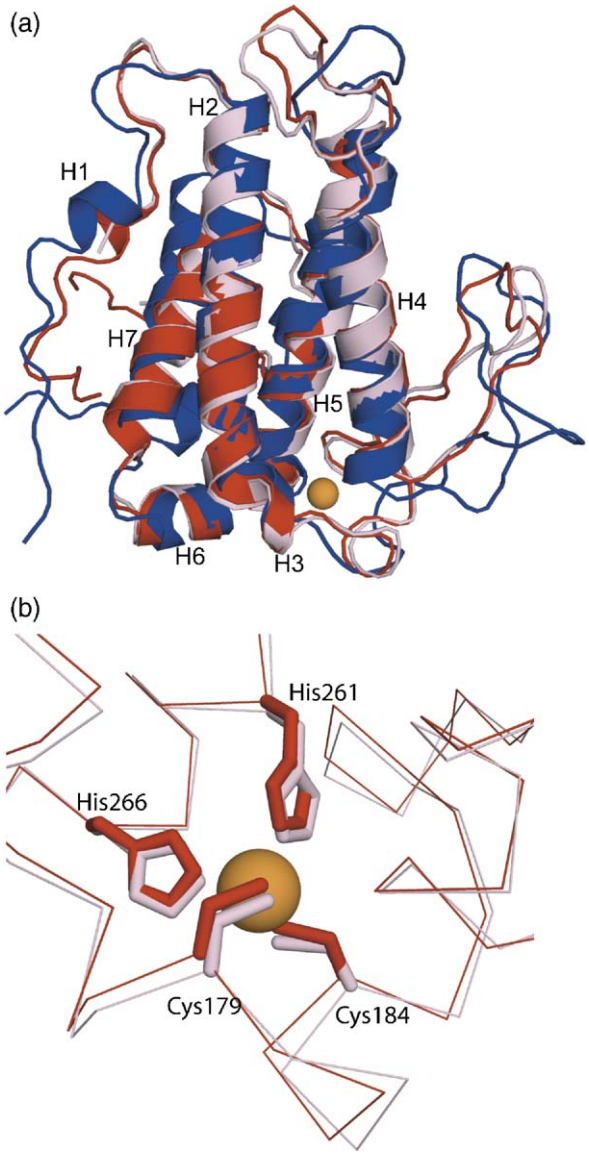

Figure 3. Structural aligment of the *Xenopus*, human and *S. cerevisiae* Mob1 cores and zinc-binding sites. (a) Superposition of the *Xenopus* (in blue), human (in red) and *S. cerevisiae* (in pink) Mob1 core structures. *S. cerevisiae* Mob1 structure RMSD *versus* human Mob1 = 0.86 Å; RMSD *versus Xenopus* Mob1 = 1.46 Å. (b) Superposition of the human (in red) and *S. cerevisiae* (in pink) zinc-binding sites. Residues coordinating zinc binding are shown in stick representation.

of sufficient length to allow helix H0 to bind to the core domain in an intramolecular manner, suggesting that the interdigitated dimer may be of physiological relevance. It is important to note that the distance constraint imposed by three disordered residues linking helix H0 and the Mob1 core is satisfied unambiguously by H0 binding to the core of a single symmetry-related Mob1 molecule, as displayed in Figure 2.

Strand S-1 (residues 82–84) binds in an antiparallel fashion to strand β2, forming an extension of the β sheet composed by strands β2 and β1 (Figure 2). The linker joining strands S-1 and S0 (residues 86–97) was disordered and could not be modeled. Due to the length of the disordered region, it is feasible that strand S-1 associates with the Mob1 core in an intramolecular manner (as shown in Figure 2) or in an intermolecular manner (not shown). Sequence conservation suggests that strand S-1 is unique to fungal species in the Mob1A subgroup (Figure 1).

Dimer interface

The dimerization of ScMob1 buries a total surface area of 3011 Å^2. The dimerization interface can be subdivided into two physically distinct components. The first consists of the association of the amphipathic helix H0 with a shallow hydrophobic depression that is conserved in the Mob1 core. This shallow depression is formed by Tyr263, Cys264, Phe267, Leu271, Asn280, Pro303, Leu304, Leu307 and Leu311 (Figure 4(a)). Of these residues, Tyr263, Phe267, Asn280, Leu304, Leu307 and Leu311 are well conserved across the Mob1 and Mob2 groups, while only Tyr263 and Leu304 are well conserved in the Mob3 group. The remainder of the surface is highly conserved within the Mob3 group itself. The predominantly hydrophobic face of helix H0 engages the Mob1 core through residues Ile127, Ile130, Val131, Met133, Thr134, Leu135 and Glu138. (note that the side-chain for residue 138 was not modeled beyond Cβ due to disorder). The total buried surface area for the helix to core interaction is 870 A^2. Importantly, the amphipathic nature of helix H0 is conserved amongst the Mob1A, 1B and Mob2A subgroups, even though the actual sequence of helix H0 varies considerably across the three subgroups. Within the Mob1A subgroup, the buried hydrophobic residues are invariant, while in the Mob1B subgroup, conservative substitutions of the hydrophobic positions are present. In the Mob2A subgroup, the corresponding hydrophobic residues diverge but are still well conserved amongst their subgroup. An analogous amphipathic helix H0 is not obvious in the Mob2B or Mob3 subgroups.

The second dimer contact region, which buries 1270 Å^2 of surface area, is mediated by direct interaction of two Mob1 cores through a combination of hydrophobic and hydrophilic contacts. The core-to-core contact surface is composed of helices H2, H3, H6, H7, the H6- H7 linker region, and a minor contribution from strand S0. Hydrophobic dimer contact residues include Met170, Phe178, Leu273, Leu275 and Val278 (Figure 4(b)). The majority of these residues are conserved across most Mob1 and Mob2 proteins. A total of three hydrogen bonds defined the core-to-core dimer interface of ScMob1: Gln167 to the backbone carbonyl of Leu273, Glu177 to the backbone amide of His108 and Glu272 to the side-chain of His108 (Figure 4(b)). These hydrogen bonded residues are maintained within the Mob1A subgroup and, while less conserved across the three main subgroups, conservation of residues at the corresponding positions

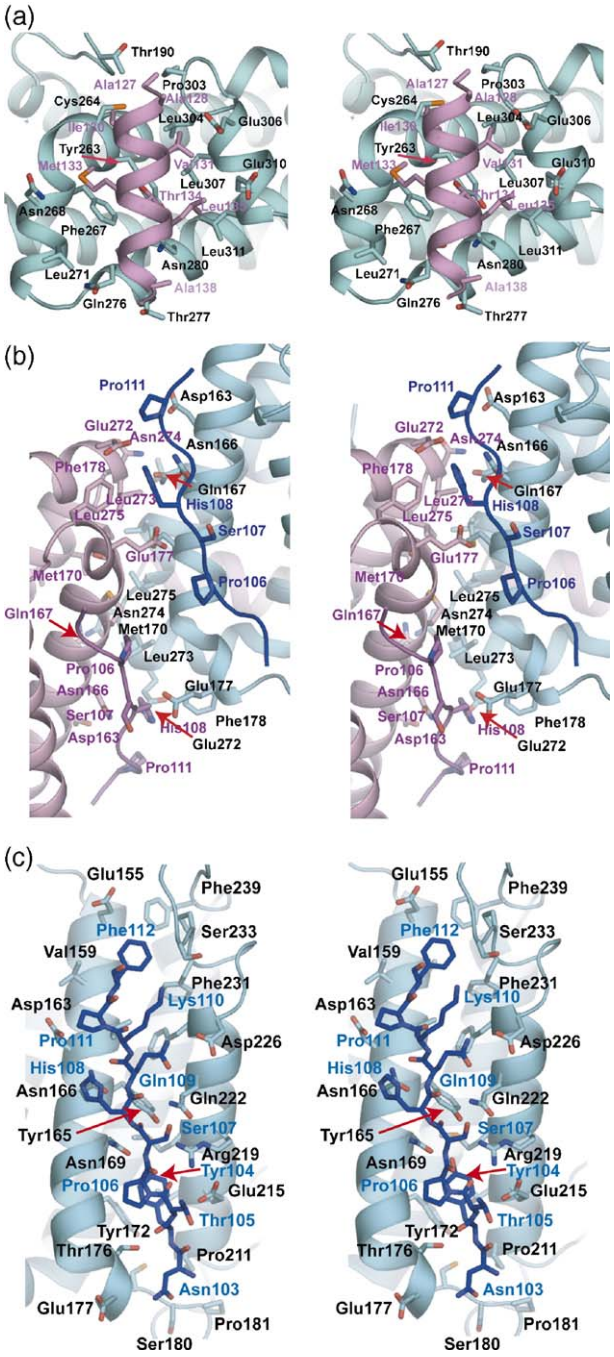

Figure 4. The helix H0– Mob1 core interaction, the core-core dimerization interface, and the strand S0-Mob1 core interaction. (a) Stereo representation of the helix H0–Mob1 core interaction. The ribbon diagram of helix H0 is shown in pink and the binding pocket on the Mob1 core is shown in blue. Interface residues on helix H0–Mob1 core interface are labeled. (b) Stereo representation of the core-core dimerization interface. One Mob1 protomer is in pink with strand S0 highlighted in magenta, and the second protomer is in blue with strand S0 highlighted in dark blue. Residues at the core–core interface are labeled. (c) Stereo representation of the strand S0–Mob1 core interaction. A stick representation of strand S0 is shown in dark blue, and the binding pocket on the Mob1 core is in blue as a ribbon diagram. Residues at the strand S0–Mob1 core interface are labeled.

within the subgroups suggests conserved function. The observed variation of hydrophobic and hydrophilic dimer interface residues might enable specific homo or hetero-dimerization of specific Mob family members.

Intramolecular strand interactions

The extended strand S0 binds across the ScMob1 core in an intramolecular manner (Figure 2). Two notable aromatic residues, Tyr104 and Phe112, anchor each end of the S0 strand by binding two hydrophobic pockets on the ScMob1 core. The Tyr104 binding pocket is composed of Asn169, Tyr172, Thr176, Val214 and Met218, while the Phe112 binding pocket is composed of Glu155, Val159, Phe225, Phe231, Ser233 and Phe239 (Figure 4(c)). These two binding pockets are conserved across the Mob1 and Mob2 groups. The spacer sequence between the anchor residues is poorly conserved. However, the mode of binding of strand S0 to the Mob1 core appears to occur in a sequence-independent manner, as out of 13 total hydrogen bonds between strand S0 and the Mob1 core, eight occur with the backbone of strand S0. The hydrogen bonded side-chains on the Mob1 core are well conserved within Mob subgroups. The conservation of the hydrophobic anchor positions and the sequence-independent nature of the majority of hydrogen bonds to strand S0 suggest that the intramolecular binding mode of strand S0 may be feasible for most proteins within the Mob1A and Mob1B subgroups.

We note that strand S0 covers the putative Dbf2 binding site on Mob1, as mapped by Mob1 temperature-sensitive alleles,[22] and by NMR analyses.[21] Some of the temperature-sensitive mutations on this surface including those encoded by mob1-55 (T85P, Q167R, Y183H), mob1-77 (E151K), mob1-95 (L157P, A158I) disrupt binding to Dbf2.[2] The intramolecular association of strand S0 with the Mob1 core domain may thus regulate the Mob1–Dbf2 interaction.

Testing novel N-terminal elements of ScMob1 *in vivo*

The novel structural elements observed in the *S. cerevisiae* Mob1$^{79\text{-}314}$ structure were then tested for relevance by complementation of *MOB1* function in yeast. Wild-type and mutant variants of Mob1$^{79\text{-}314}$ were assessed for their ability to complement a *mob1* deletion strain under different Mob1 protein expression levels and growth temperatures. In the absence of Mob1 protein (Figure 5, row1), yeast were not viable under all conditions tested. However, Mob1$^{1\text{-}314}$ expressed under the control of its endogenous promoter is viable under all conditions tested (row 2). All Mob1$^{79\text{-}314}$ constructs used in this study were driven by the GAL1 promoter in order to regulate expression on various carbon sources. As reported, we find that Mob1$^{79\text{-}314}$ is viable under all conditions tested (row 3 and (A)), indicating that the

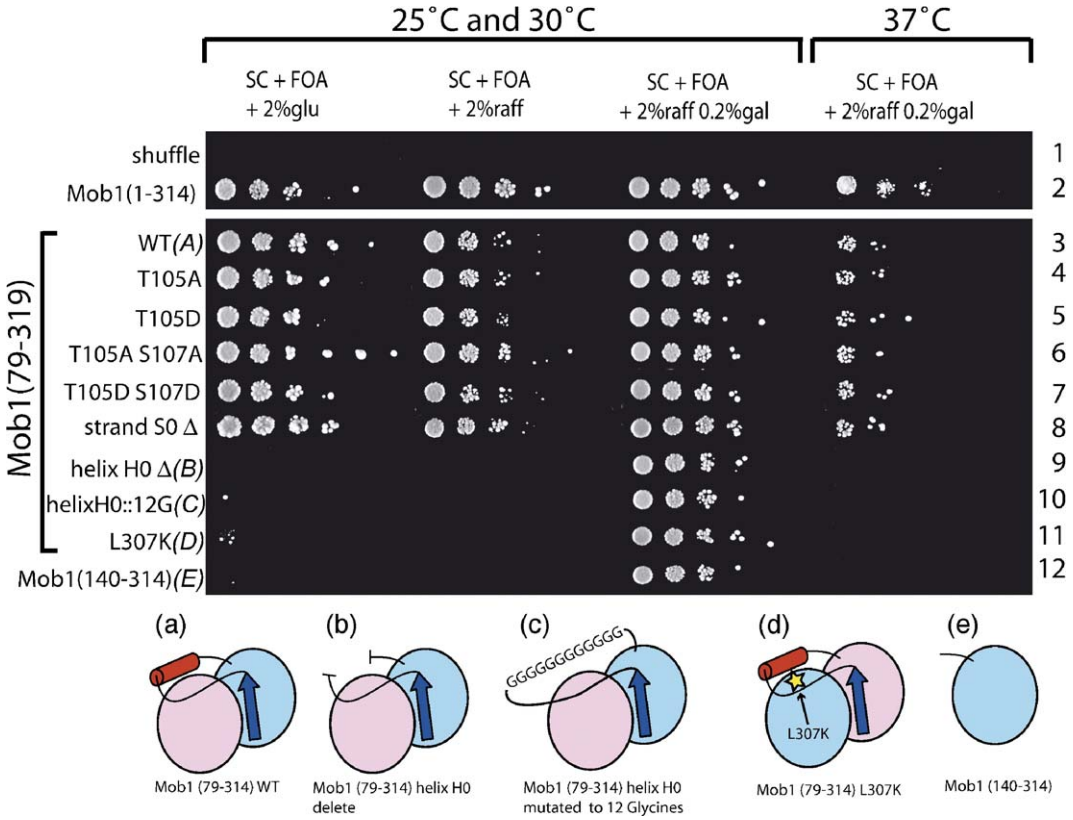

Figure 5. Mob1 complementation. Complementation of a *mob1*Δ*kan* strain was used to test ther functional importance of novel elements in *S. cerevisiae* Mob1$^{79\text{-}314}$. Mob1$^{79\text{-}314:\ WT}$ and Mob1$^{79\text{-}314}$ mutants were cloned under the GAL1 promoter and tested for growth at different temperatures (25 °C, 30 °C and 37 °C) and carbon sources (2% (w/v) glucose, 2% (w/v) raffinose and 2% (w/v) raffinose + 0.2% (w/v) galactose). In the absence of Mob1 protein (shuffle vector alone), yeast were inviable under all conditions tested (row 1). Mob1$^{1\text{-}314}$ expressed from the endogenous *MOB1* promoter was viable under all conditions tested (row 2). Mob1$^{79\text{-}314}$ was also viable under all conditions tested (row 3). The Mob1 core, Mob1$^{140\text{-}314}$ did not fully complement the *mob1*Δ*kan* strain (row 12). Mutations in strand S0, including Mob1$^{79\text{-}314:\ T105A}$ (row 4), Mob1$^{79\text{-}314:\ T105D}$ (row 5), Mob1$^{79\text{-}314:\ T105A\ \&\ S107A}$ (row 6), Mob1$^{79\text{-}314:\ T105D\ \&\ S107D}$ (row 7) and Mob1$^{79\text{-}314:\ strand\ S0\Delta}$ (row8) fully complemented the *mob1*Δ*kan* strain. Mutations in helix H0 and its binding pocket on the Mob1 core, including Mob1$^{79\text{-}314:\ helix\ H0\Delta}$ (row 9), Mob1$^{79\text{-}314:\ helix\ H0\rightarrow 12Gly}$ (row10) and Mob1$^{79\text{-}314:\ L307K}$ (row 11), did not complement the *mob1*Δ*kan* strain under conditions of lower expression or higher temperature.

unique, *S. cerevisiae* specific N-terminal 78 amino acid residue region is not functionally important under the conditions tested. In contrast, the Mob1 core (Mob1$^{140\text{-}314}$) does not complement, except when the level of protein expression is increased and temperature is decreased (row 12, column 3 and (E)). These results demonstrate that the cell is very sensitive to Mob1 levels, and that the lethal phenotype resulting from the deletion of the N-terminal region can be offset by increased levels of protein expression and lower temperature.

To assess functionality within the N-terminal region, we generated mutations in each defined motif and determined the relative contributions to cell viability. Deletion of the strand S0 in Mob1 (Mob1$^{79\text{-}314\Delta S0}$) is dispensable for viability (row 8). As Mob1 is a phospho-protein, we focused on the possibility that strand S0 association with the core was regulated in a phosphorylation-dependent manner. As such, the two conserved strand S0 residues Ser107 and Thr105 were mutated to aspartic acid to mimic phosphorylation and to alanine to block phosphorylation at these sites. We found that all single and double site mutants within strand S0 had no discernable effect on cell viability (rows 4–7).

In contrast, deletion of the helix H0 (Mob1$^{79\text{-}314\Delta H0}$) and replacement of the helix H0 with a polyglycine tract (Mob1$^{79\text{-}314H0\rightarrow 12GLY}$) abrogates viability under all conditions except when protein expression level is increased and temperature is decreased (rows 9 and 10, and (B), (C)) Interestingly, a reciprocal mutation on Mob1 core, Mob1^{L307K}, that was designed to prohibit helix H0 binding had the same effect on yeast viability (row 11 and (D)). These results indicate that there is an essential function for the Mob1 helix H0 and the reciprocal helix H0 binding site on the Mob1 core.

Discussion

Structure of ScMob1$^{79\text{-}314}$

Two structures of Mob1 proteins corresponding to the highly conserved protease-resistant Mob1 core

(residues 140–314 in ScMob1) have been reported.[21,22] Sequence conservation indicates that all Mob proteins will adopt highly similar core structures and, indeed, we observe this to be the case for *S. cervisiae* Mob1. The N-terminal region (corresponding to residues 79–140 of ScMob1) of Mob proteins is not highly conserved but patterns of conservation are evident within Mob protein groups (Mob1, Mob2, Mob3) that parallel subtle sequence differences within their core domains. Here, we have solved the X-ray crystal structure of ScMob1$^{79\text{-}314}$ which provides a first look at the N-terminal region of a Mob protein. The ScMob1$^{79\text{-}314}$ structure revealed three novel structural elements in the N terminus; namely, strand S-1, strand S0 and helix H0. Strand S-1 forms an extension of the sheet composed by strands β1 and β2. Strand S0 binds in an intramolecular manner to the C-terminal core domain across the putative Dbf2 binding site mapped previously by Mob1 temperature-sensitive mutations and NMR.[21,22] While strand S0 is not highly conserved in sequence across all Mob proteins, the sequence-independent nature of the strand S0 mode of binding to the C-terminal core domain suggests that this may be a more general feature of the Mob proteins.

The third structural element of the N-terminal region of ScMob1$^{79\text{-}314}$ consists of an ampiphathic α-helix, denoted H0. Helix H0 engages a second Mob1 molecule in an intermolecular manner, thus contributing to molecular dimerization. The notion that helix H0 is important for Mob1 homodimerization is supported, in part, by the observation that previous human[22] and *Xenopus*[21] structures of Mob1 corresponding to the core domain were monomeric, while our larger ScMob1 crystallization construct forms dimers in solution (as evidenced by static light-scattering analysis) and within the crystal environment. Sequence conservation suggests that the presence of helix H0 may be a common feature of Mob1A, Mob1B and Mob2A protein subgroups but not Mob2B and Mob3 subgroups. Although sequence conservation suggests that the latter Mob protein sub-groups do not possess either strand S0 or helix H0 structural elements within their N-terminal regions, the high degree of conservation may indicate the presence of alternative structural features.

Functional analysis of N-terminal region

Consistent with previously reported results,[2] we find that the Mob1 core is not able to fully complement Mob1 function. In order to identify the functionally important regions within the N-terminal region of Mob1, we generated a variety of mutants that selectively affected helix H0 and strand S0. Interestingly, we found that deletion of helix H0 or replacement of helix H0 with 12 glycine residues on Mob1 compromises its ability to fully complement function. Furthermore, the predicted disruption of helix H0 binding to the Mob1 core caused by introduction of a point mutation (Mob1^{L307K}) in the helix H0 binding pocket also disrupts the ability of the protein to fully complement. Together, these results indicate that the protein sequence corresponding to helix H0 is functionally important. In addition, the finding that the L307K mutation in the helix H0 binding pocket had the same effect on yeast viability as the helix H0 deletion supports the possibility that helix H0 binds to the core domain in the same manner as that revealed by the ScMob1$^{79\text{-}314}$ crystal structure *in vivo*.

Based on the position of strand S0 in the putative Dbf2 binding site on the Mob1 core, we tested whether strand S0 plays an auto-inhibitory role. Previously studied mechanisms of kinase auto-inhibition have shown that phosphorylation of regulatory elements commonly serves to relieve auto-inhibition.[23] To test if this strand S0 is an auto-inhibitory element regulated by phosphorylation, we mutated the conserved Ser107 and Thr105 on strand S0 to alanine and aspartic acid to block phosphorylation at these positions and mimic phosphorylation at these residues, respectively. However, none of the single or double mutants had an effect under the conditions tested. While this result does not rule out the possibility that strand S0 is an auto-inhibitory element, our results indicate that phosphorylation at Ser107 or Thr105 is not required for protein function. Because deletion of strand S0 does not have an overt effect on viability, more sensitive assays may be required to discern an auto-inhibitory role of strand S0. These studies reveal novel structural elements that may contribute to Mob1 and/or Dbf2/20 regulation *in vivo*.

Dimerization of Mob1 *in vivo*

Our functional studies support the possibility that Mob1 may adopt the dimer configuration *in vivo*. However, we have not been able to demonstrate homodimerization of Mob1 by co-immunoprecipitation experiments *in vivo* (Supplementary Data Figure 3a). While this result raises the possibility that Mob1 does not homodimerize *in vivo*, it is possible that Mob1 homodimerization is transient and occurs only at specific times in the cell cycle. As such, more sensitive assays may be required to detect dimerization.

Interestingly, immunoprecipitation experiments reveal that Mob1 interacts with Mob2 in *S. cerevisiae in vivo* (Supplementary Data Figure 3b). This interaction appears direct, as bacterially expressed Mob1 and Mob2 also interact *in vitro* (Supplementary Data Figure 3c). The fact that the Mob1 and Mob2 cores are very similar (Figure 1) and that helix H0 appears to be conserved in Mob2, raises the intriguing possibility that the ScMob1 homodimer structure may have relevance to Mob1-Mob2 heterodimer formation. Consistent with this possibility, the core domain of Mob1 (Mob1$^{140\text{-}314}$) and a Mob1 mutant in which helix H0 was selectivity deleted (Mob1$^{79\text{-}314\Delta H0}$), do not interact with Mob2 *in vivo* (Supplementary Data Figure 3d, lanes 14 and 13). While the poor expression of the Mob1 core could

account for a lack of binding to Mob2, the level of expression of the Mob1 helix H0 delete was comparable to that of the longer Mob1$^{79\text{-}314}$ protein (Supplementary Data Figure 3d, lanes 13 and 12). A structural analysis of a Mob1-Mob2 hetero complex will be required to fully discern its relation to the Mob1 homodimer.

Materials and Methods

Protein expression, mutagenesis and purification

The *S. cerevisiae* Mob1 protein corresponding to residues 79–314 was expressed in *Escherichia coli* as a GST-fusion protein using the pGEX-2T vector (Pharmacia). Bacterial pellets were lysed in a solution containing 1.34 M NaCl, 2.7 mM KCl, 10 mM Na_2HPO_4 (pH 7.3). Protein was purified using glutathione-Sepharose affinity chromatography and eluted by TEV protease cleavage. Eluted protein was concentrated and loaded onto a Superdex-75 size-exclusion column (sizing column buffer = 100 mM Hepes (pH 7.5), 150 mM NaCl, 1 mM DTT). To obtain a selenomethionyl derivative of Mob1$^{79\text{-}314}$, *E. coli* B834 cells were transformed and grown in minimal medium supplemented with selenomethionine and ampicillin. The Quickchange kit (Stratagene) was used to generate the Mob1 mutants. Expression and purification of the mutants was performed as described above for the native Mob1$^{79\text{-}314}$ protein.

Table 1. Data collection, structure determination and refinement statistics

Crystal			
Space group	*C*2 monoclinic		
Cell dimensions			
a (Å)	72.75		
b (Å)	70.81		
c (Å)	50.62		
β (deg.)	119.35		
Data (SeMet MAD)	Inflection	Peak	Remote
Wavelength (Å)	0.9795	0.9792	0.9600
Resolution (Å)	2.05	2.05	2.02
Reflections			
Total	40,315	36,788	45,433
Unique	14,583	14,641	15,846
Completeness (%)	97.4 (96.7)	98.5 (98.5)	96.9 (94.2)
I/σ	11.8 (3.1)	14.2 (3.7)	12.4 (3.9)
R_{sym}	8.6 (27.5)	7.0 (21.2)	6.4 (21.5)
Refinement statistics			
Resolution range (Å)	35.0 – 2.0		
R_{factor}	0.202		
R_{free}	0.237		
r.m.s. deviation			
Bond angles (deg)	1.760		
Bond lengths (Å)	0.020		
Protein atoms	1656		
Zn atoms	1		
Water molecules	92		
Average *B*-factors (Å^2)			
Main chain	22.9		
Side chain	24.6		
Solvent	31.6		
Ramachandran plot			
Most favored regions (%)	93.8		
Allowed regions (%)	5.6		
Generously allowed regions (%)	0.6		
Disallowed regions (%)	0.0		

Values in parentheses are for reflections in the highest resolution bin.

Table 2. *Saccharomyces cerevisiae* strains used in this study

Strain[a]	Genotype	Source
BY4741	MATa *leu2 his3 ura3 met15*	28
MT3738	MATa/α*leu2/leu2 his3/his3 ura3/ura3 MOB1/mob1*Δ*kan*[28b]	
MT3739	MATa *leu2 his3 ura3 mob1*Δ*kan <CEN MOB1-URA3>*	This study[c]

[a] All strains are derived from the S288c background.
[b] Obtained from Deletion Set Consortium strain collection. Confirmed by PCR amplification and sequencing of gene-specific tags.
[c] Constructed by sporulation and tetrad dissection of MT3738. Deletion of *MOB1* was covered with a centromeric plasmid expressing *MOB1*.

Mob1 crystallization, data collection and structure determination

Hanging drops containing 1 μl of 25 mg/ml of selenomethionyl derivative protein in 100 mM Hepes (pH 7.5), 150 mM NaCl, 1 mM DTT was mixed with equal volumes of reservoir buffer containing 100 mM Mes (pH 6.0), 1.2 M ammonium sulfate. Elongated crystals were obtained after two to three days at 4 °C. Flash-freezing of the crystals was performed using the crystallization buffer complemented with 25% (v/v) ethylene glycol. Multi-wavelength anomalous diffraction (MAD) diffraction data was collected on frozen crystals at the Brookhaven National Laboratories on X8-C beamline and data processing was carried out using HKL2000.[24] Heavy-atom identification, phasing information and experimental electron density map calculation was performed using SHARP.[25] Model building and refinement were carried out using O[26] and CNS.[27] Refinement statistics are summarized in Table 1. The first two residues (79-80), the S-1 to S0 linker (residues 86–97), the S0 to H0 linker (residues 113–125), the H0 to core linker (residues 140–142) as well as the last residue (314) in the Mob1 construct were disordered and hence could not been modeled. No side-chain electron density was observed for residues 98, 126, 128, 132, 200, 246, 312 or 313, so they were modeled as alanine in the final structure.

Table 3. Mob1 mutants used in this study

Strain	Relevant characteristics	Source
pMT3630	*MOB1*$^{1\text{-}314}$ *URA3 CEN*	A. Amon
pMT3959	*MOB1*$^{1\text{-}314}$ *HIS3 CEN*	This study
pSM28	*pGAL-MOB1*$^{79\text{-}314}$ *HIS3 CEN*	This study
pSM31	*pGAL-MOB1*$^{79\text{-}314:\ strand\ S0\Delta}$ *HIS3 CEN*	This study
pSM32	*pGAL-MOB1*$^{79\text{-}314:\ T105D}$ *HIS3 CEN*	This study
pSM33	*pGAL-MOB1*$^{79\text{-}314:\ T105A}$ *HIS3 CEN*	This study
pSM34	*pGAL-MOB1*$^{79\text{-}314:\ helix\ H0\Delta}$ *HIS3 CEN*	This study
pSM37	*pGAL-MOB1*$^{79\text{-}314:\ T105A,\ S107A}$ *HIS3 CEN*	This study
pSM38	*pGAL-MOB1*$^{140\text{-}314}$ *HIS3 CEN*	This study
pSM44	*pGAL-MOB1*$^{79\text{-}314:\ helix\ H0::12G}$ *HIS3 CEN*	This study
pSM53	*pGAL-MOB1*$^{79\text{-}314:\ T105D,\ S107D}$ *HIS3 CEN*	This study
pSM56	*pGAL-MOB1*$^{79\text{-}314:\ L307K}$ *HIS3 CEN*	This study

Mob1 complementation

A *mob1* shuffle strain was constructed by sporulating a MOB1/*mob1*Δ*kan* heterozygous diploid from the Euroscarf deletion set and isolating kanamycin-resistant segregants, which were rendered viable by a 3.6 kb BamH1 fragment of *MOB1* in a <*URA3 CEN*> plasmid. The 3.6 kb *MOB1* fragment was also subcloned into a <*HIS3 CEN*> plasmid as a template for mutagenesis. All yeast strains used in this study are listed in Table 2. Complementation of the shuffle strain by various <MOB1 ^{mutant}HIS *CEN*> plasmids was tested by plating on synthetic complete medium containing 0.1% FOA. Briefly, 10^6 cells were serially diluted in tenfold increments and spotted onto medium containing 2% (w/v) glucose, 2% (w/v) raffinose, 2% (w/v) raffinose + 0.2% (w/v) galactose and incubated at 25 °C, 30 °C and 37 °C. Cells were photographed after four days of growth. Mob1 mutants used in the complementation assay are listed in Table 3.

Protein Data Bank accession number

The ScMob1$^{79\text{-}314}$ coordinates and structure factors have been deposited in the Protein Data Bank with the accession number 2HJN.

Acknowledgements

We thank the beamline staff at Brookhaven National Laboratories X8-C beamline where diffraction data were collected. We thank Jessica Ahn for assistance with PCR. L.B. is a research student of the Terry Fox Foundation through an award from the National Cancer Institute of Canada. This work was supported by grants from the National Cancer Institute of Canada and Canadian Institutes of Health Research to F.S. and M.T.

Supplementary Data

Supplementary data associated with this article can be found, in the online version, at doi:10.1016/j.jmb.2006.07.007

References

1. Luca, F. C. & Winey, M. (1998). MOB1, an essential yeast gene required for completion of mitosis and maintenance of ploidy. *Mol. Biol. Cell*, **9**, 29–46.
2. Komarnitsky, S. I., Chiang, Y. C., Luca, F. C., Chen, J., Toyn, J. H., Winey, M. *et al.* (1998). DBF2 protein kinase binds to and acts through the cell cycle-regulated MOB1 protein. *Mol. Cell Biol.* **18**, 2100–2107.
3. Lee, S. E., Frenz, L. M., Wells, N. J., Johnson, A. L. & Johnston, L. H. (2001). Order of function of the budding-yeast mitotic exit-network proteins Tem1, Cdc15, Mob1, Dbf2, and Cdc5. *Curr. Biol.* **11**, 784–788.
4. Mah, A. S., Jang, J. & Deshaies, R. J. (2001). Protein kinase Cdc15 activates the Dbf2-Mob1 kinase complex. *Proc. Natl Acad. Sci. USA*, **98**, 7325–7330.
5. Justice, R. W., Zilian, O., Woods, D. F., Noll, M. & Bryant, P. J. (1995). The Drosophila tumor suppressor gene warts encodes a homolog of human myotonic dystrophy kinase and is required for the control of cell shape and proliferation. *Genes Dev.* **9**, 534–546.
6. Xu, T., Wang, W., Zhang, S., Stewart, R. A. & Yu, W. (1995). Identifying tumor suppressors in genetic mosaics: the Drosophila lats gene encodes a putative protein kinase. *Development*, **121**, 1053–1063.
7. Zallen, J. A., Peckol, E. L., Tobin, D. M. & Bargmann, C. I. (2000). Neuronal cell shape and neurite initiation are regulated by the Ndr kinase SAX-1, a member of the Orb6/COT-1/warts serine/threonine kinase family. *Mol. Biol. Cell*, **11**, 3177–3190.
8. Jeffrey, P. D., Russo, A. A., Polyak, K., Gibbs, E., Hurwitz, J., Massague, J. & Pavletich, N. P. (1995). Mechanism of CDK activation revealed by the structure of a cyclinA-CDK2 complex. *Nature*, **376**, 313–320.
9. Morgan, D. O. (1996). The dynamics of cyclin dependent kinase structure. *Curr. Opin. Cell Biol.* **8**, 767–772.
10. Nasmyth, K. (1996). At the heart of the budding yeast cell cycle. *Trends Genet.* **12**, 405–412.
11. Morgan, D. O. (1997). Cyclin-dependent kinases: engines, clocks, and microprocessors. *Annu. Rev. Cell Dev. Biol.* **13**, 261–291.
12. Bardin, A. J. & Amon, A. (2001). Men and sin: what's the difference? *Nature Rev. Mol. Cell Biol.* **2**, 815–826.
13. Nelson, B., Kurischko, C., Horecka, J., Mody, M., Nair, P., Pratt, L. *et al.* (2003). RAM: a conserved signaling network that regulates Ace2p transcriptional activity and polarized morphogenesis. *Mol. Biol. Cell*, **14**, 3782–3803.
14. Weiss, E. L., Kurischko, C., Zhang, C., Shokat, K., Drubin, D. G. & Luca, F. C. (2002). The *Saccharomyces cerevisiae* Mob2p-Cbk1p kinase complex promotes polarized growth and acts with the mitotic exit network to facilitate daughter cell-specific localization of Ace2p transcription factor. *J. Cell Biol.* **158**, 885–900.
15. Ito, T., Chiba, T., Ozawa, R., Yoshida, M., Hattori, M. & Sakaki, Y. (2001). A comprehensive two-hybrid analysis to explore the yeast protein interactome. *Proc. Natl Acad. Sci. USA*, **98**, 4569–4574.
16. Devroe, E., Erdjument-Bromage, H., Tempst, P. & Silver, P. A. (2004). Human Mob proteins regulate the NDR1 and NDR2 serine-threonine kinases. *J. Biol. Chem.* **279**, 24444–24451.
17. Lai, Z. C., Wei, X., Shimizu, T., Ramos, E., Rohrbaugh, M., Nikolaidis, N. *et al.* (2005). Control of cell proliferation and apoptosis by mob as tumor suppressor, mats. *Cell*, **120**, 675–685.
18. He, Y., Emoto, K., Fang, X., Ren, N., Tian, X., Jan, Y. N. & Adler, P. N. (2005). Drosophila Mob family proteins interact with the related Tricornered (Trc) and Warts (Wts) Kinases. *Mol. Biol. Cell.* **16**, 4139–4152.
19. St John, M. A., Tao, W., Fei, X., Fukumoto, R., Carcangiu, M. L., Brownstein, D. G. *et al.* (1999). Mice deficient of Lats1 develop soft-tissue sarcomas, ovarian tumours and pituitary dysfunction. *Nature Genet.* **21**, 182–186.
20. McPherson, J. P., Tamblyn, L., Elia, A., Migon, E., Shehabeldin, A., Matysiak-Zablocki, E. *et al.* (2004). Lats2/Kpm is required for embryonic development, proliferation control and genomic integrity. *EMBO J.* **23**, 3677–3688.
21. Ponchon, L., Dumas, C., Kajava, A. V., Fesquet, D. &

Padilla, A. (2004). NMR solution structure of Mob1, a mitotic exit network protein and its interaction with an NDR kinase peptide. *J. Mol. Biol.* **337**, 167–182.
22. Stavridi, E. S., Harris, K. G., Huyen, Y., Bothos, J., Verwoerd, P. M., Stayrook, S. E. *et al.* (2003). Crystal structure of a human Mob1 protein: toward understanding Mob-regulated cell cycle pathways. *Structure (Camb)*, **11**, 1163–1170.
23. Wybenga-Groot, L. E., Baskin, B., Ong, S. H., Tong, J., Pawson, T. & Sicheri, F. (2001). Structural basis for autoinhibition of the Ephb2 receptor tyrosine kinase by the unphosphorylated juxtamembrane region. *Cell*, **106**, 745–757.
24. Otwinowski, Z. & Minor, W. (1997). Processing of X-ray diffraction data collected in oscillation mode. *Methods Enzymol.* **276**, 307–326.
25. de La Fortelle, E. & Bricogne, G. (1997). Maximum-likelihood heavy-atom parameter refinement for multiple isomorphous replacement and multiwavelength anomalous diffraction methods. *Methods Enzymol.* **276**, 472–494.
26. De Bondt, H. L., Rosenblatt, J., Jancarik, J., Jones, H. D., Morgan, D. O. & Kim, S. H. (1993). Crystal structure of cyclin-dependent kinase 2. *Nature*, **363**, 595–602.
27. Brunger, A. T., Adams, P. D., Clore, G. M., DeLano, W. L., Gros, P., Grosse-Kunstleve, R. W. *et al.* (1998). Crystallography & NMR system: A new software suite for macromolecular structure determination. *Acta Crystallog. sect. D*, **54**, 905–921.
28. Brachmann, C. B., Davies, A., Cost, G. J., Caputo, E., Li, J., Hieter, P. & Boeke, J. D. (1998). Designer deletion strains derived from *Saccharomyces cerevisiae* S288C: a useful set of strains and plasmids for PCR-mediated gene disruption and other applications. *Yeast*, **14**, 115–132.

Edited by I. Wilson

(Received 26 April 2006; received in revised form 1 July 2006; accepted 6 July 2006)
Available online 24 August 2006